

## Field-Induced Slow Magnetic Relaxation in a Six-Coordinate Mononuclear Cobalt(II) Complex with a Positive Anisotropy

Julia Vallejo,<sup>†</sup> Isabel Castro,<sup>†</sup> Rafael Ruiz-García,<sup>†,‡</sup> Joan Cano,<sup>\*,†,‡</sup> Miguel Julve,<sup>†</sup> Francesc Lloret,<sup>†</sup> Giovanni De Munno,<sup>§</sup> Wolfgang Wernsdorfer,<sup>||</sup> and Emilio Pardo<sup>\*,†</sup>

<sup>†</sup>Instituto de Ciencia Molecular (ICMOL), Universitat de València, 46980 Paterna, València, Spain

<sup>‡</sup>Fundació General de la Universitat de València (FGUV), Universitat de València, 46980 Paterna, València, Spain

<sup>§</sup>CEMIF.CAL, Dipartimento di Chimica, Università degli Studi della Calabria, 87030 Cosenza, Italy

<sup>||</sup>Institut Néel, CNRS, Nanoscience Department, BP 166, 380412 Grenoble Cedex 9, France

### Supporting Information

**ABSTRACT:** The novel mononuclear Co(II) complex *cis*-[Co<sup>II</sup>(dmphen)<sub>2</sub>(NCS)<sub>2</sub>] $\cdot$ 0.25EtOH (**1**) (dmphen = 2,9-dimethyl-1,10-phenanthroline) features a highly rhombically distorted octahedral environment that is responsible for the strong positive axial and rhombic magnetic anisotropy of the high-spin Co<sup>II</sup> ion ( $D = +98 \text{ cm}^{-1}$  and  $E = +8.4 \text{ cm}^{-1}$ ). Slow magnetic relaxation effects were observed for **1** in the presence of a dc magnetic field, constituting the first example of field-induced single-molecule magnet behavior in a mononuclear six-coordinate Co(II) complex with a transverse anisotropy energy barrier.

The observation of slow magnetic relaxation effects in mononuclear rare-earth complexes constituted a major achievement in the emerging field of molecular nanomagnetism.<sup>1</sup> Until then, scientists' efforts had been devoted to the synthesis of polynuclear complexes with the highest possible ground-state spin ( $S$ ) and negative axial magnetic anisotropy ( $D$ )<sup>2</sup> in order to get the largest energy barrier ( $E_a$ ) for the magnetization reversal between the two lowest  $M_S = \pm S$  states [ $E_a = -DS^2$  and  $-D(S^2 - 1/4)$  for integer and half-integer spins, respectively].<sup>3</sup> Mononuclear complexes with a single slow-relaxing metal center, so-called single-ion magnets (SIMs), have emerged as simpler model systems for fundamental research on magnetic relaxation dynamics from both the experimental and theoretical points of view. As polynuclear single-molecule magnets (SMMs),<sup>4</sup> SIMs are also a major scientific target because of their potential applications in high-density magnetic memories and quantum-computing devices.

Since the first publication of slow magnetic relaxation in double-decker bis(phthalocyaninato)terbium(III)<sup>1a</sup> and -dysprosium(III)<sup>1b</sup> complexes, only a few examples of SIMs with 3d metal ions have been reported very recently.<sup>5,6</sup> They include both four- and five-coordinate high-spin species: trigonal-pyramidal Fe(II),<sup>5</sup> tetrahedral Co(II),<sup>6a,b</sup> and square-pyramidal Co(II)<sup>6c</sup> complexes. The low coordination number in these few examples of SIMs with 3d metal ions appears to be necessary to minimize the ligand field relative to the spin-orbit coupling, allowing the desired slow magnetic relaxation effects to be observed. Here we report the novel mononuclear Co(II)

complex *cis*-[Co<sup>II</sup>(dmphen)<sub>2</sub>(NCS)<sub>2</sub>] $\cdot$ 0.25EtOH (**1**), in which dmphen is the sterically hindered ligand 2,9-dimethyl-1,10-phenanthroline. Complex **1** constitutes the very first example of a six-coordinate octahedral Co(II) complex with positive axial magnetic anisotropy ( $D > 0$ ) that exhibits field-induced slow magnetic relaxation behavior, thus enlarging the scope of SIMs with first-row transition metal ions.

Complex **1** was obtained as well-formed deep-pink parallelepipeds by slow diffusion of 1:1 (v/v) water/ethanol solutions of Co<sup>II</sup>(NCS)<sub>2</sub> and dmphen (1:2 molar ratio) in an H-shaped tube at room temperature [see the Experimental Section in the Supporting Information (SI)]. Its crystal structure consists of neutral mononuclear *cis*-[Co<sup>II</sup>(dmphen)<sub>2</sub>(NCS)<sub>2</sub>] units with pseudo-twofold molecular symmetry, together with additional disordered crystallization ethanol molecules.

The Co atom in **1** has a highly distorted six-coordinate CoN<sub>6</sub> octahedral environment wherein the two thiocyanate N atoms in *cis* positions and two imine N atoms from the two dmphen ligands define the equatorial plane while the remaining two imine N atoms occupy the axial positions (Figure 1a). The Co–N<sub>thiocyanate</sub> bond distances [2.041(3) and 2.038(3) Å] are rather shorter than the equatorial Co–N<sub>dmphen</sub> bond distances [2.275(3) and 2.255(3) Å], which are in turn slightly larger than the axial Co–N bond distances [2.188(3) and 2.194(3) Å], all of which are typical of high-spin Co<sup>II</sup> ions. Moreover, the equatorial N–Co–N bond angle involving the two *cis*-thiocyanate groups [99.9(1)°] is less bent than that involving the two dmphen ligands [80.3(1)°], and both of them deviate from the angle for an ideal octahedron (90°). The axial N–Co–N bond angle [160.4(1)°] also deviates significantly from that of an ideal octahedron (180°). This leads to an overall rhombic ( $C_{2v}$ ) distortion of the octahedral metal environment.

The large distortion of the metal environment in **1** from an ideal octahedron is explained by the occurrence of weak intramolecular  $\pi$ – $\pi$  and C–H $\cdots$  $\pi$  interactions between the methyl-substituted aromatic rings of the two dmphen ligands [the inter-ring centroid–centroid distance is 3.70(1) Å, and the hydrogen-centroid distances are 2.79 and 2.77 Å] (Figure S1 in the SI). This situation leads to an overall parallel-displaced  $\pi$ -

Received: July 31, 2012

Published: September 10, 2012

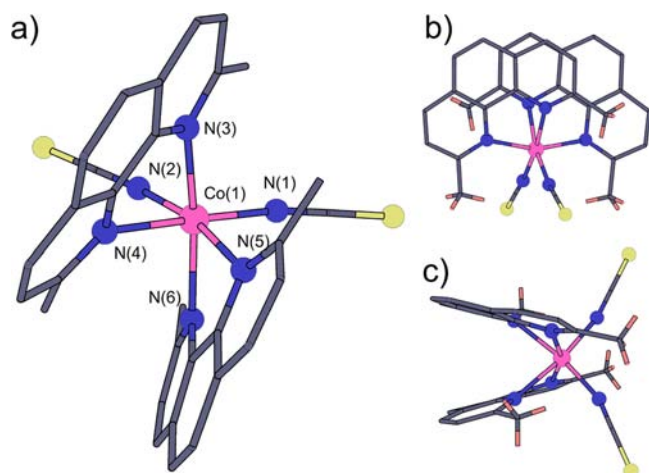


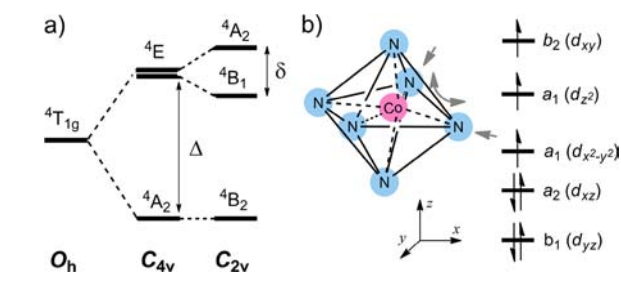
**Figure 1.** (a) Perspective view of the mononuclear Co(II) unit of **1** with the atom-numbering scheme for the metal coordination environment. (b) Top and (c) side projection views showing the parallel-displaced  $\pi$ -stacked arrangement of the dmphen ligands.

stacked arrangement reminiscent of that found in the aforementioned double-decker mononuclear lanthanides [the dihedral angle between the dmphen ligands is only  $29.8(1)^\circ$ ] (Figure 1b,c). In addition, there are weak intermolecular  $\pi$ - $\pi$  stacking interactions between the outer and/or inner aromatic rings of the dmphen ligands of neighboring centrosymmetrically related, mononuclear bis(chelated)cobalt(II) complexes [the interplanar distances are 3.47(1) and 3.56(1) Å] (Figure S2). This gives rise to heterochiral arrays of alternating  $\Lambda$ - and  $\Delta$ -Co<sup>II</sup> chiralities along the [01 $\bar{1}$ ] direction (Figure S3). However, the mononuclear units are very well isolated from each other, the shortest intermolecular Co–Co distance being 8.86(1) Å.

The direct current (dc) magnetic properties of **1** were first investigated in the form of a  $\chi_M T$  versus  $T$  plot, where  $\chi_M$  is the dc magnetic susceptibility per Co<sup>II</sup> ion (Figure S4). The  $\chi_M T$  value of  $2.83 \text{ cm}^3 \text{ mol}^{-1} \text{ K}$  at room temperature for **1** is within the range expected for one high-spin  $d^7$  Co<sup>II</sup> ion ( $S = 3/2$ ) with some orbital angular momentum contribution. Upon cooling,  $\chi_M T$  continuously decreases to a value of  $1.75 \text{ cm}^3 \text{ mol}^{-1} \text{ K}$  at 2.0 K (Figure S4), revealing the occurrence of significant spin–orbit coupling (SOC).

The magnetic susceptibility data for **1** were analyzed using a spin Hamiltonian for a mononuclear model that takes into account the SOC effects ( $S = 3/2 \Leftrightarrow L = 1$ ) by considering the well-known isomorphism between the  $T_1$  and P terms:  $\hat{H} = \alpha \lambda \hat{L} \cdot \hat{S} + \Delta [\hat{L}_z^2 - L(L+1)/3] + \delta (\hat{L}_x^2 - \hat{L}_y^2) + \beta \mathbf{H} \cdot (-\alpha \hat{L} + g_e \hat{S})$ ,<sup>7</sup> where  $\lambda$  is the spin–orbit coupling parameter,  $\alpha$  is an orbital reduction factor, and  $\Delta$  and  $\delta$  are the axial and rhombic orbital splittings of the  $T_1$  term, respectively (Scheme 1a). The least-squares fit of the magnetic susceptibility data for **1** using the VPMAG program<sup>8</sup> gave  $\lambda = -165.8 \text{ cm}^{-1}$ ,  $\Delta = +493 \text{ cm}^{-1}$ ,  $\delta = +22.5 \text{ cm}^{-1}$ , and  $\alpha = 1.225$  with  $R = 1.1 \times 10^{-5}$ , where  $R$  is the agreement factor, defined as  $R = \sum [(\chi_M T)_{\text{exptl}} - (\chi_M T)_{\text{calcd}}]^2 / \sum [(\chi_M T)_{\text{exptl}}]^2$ . The theoretical curve matched the experimental data over the whole temperature range (solid line in Figure S4). The best-fit values of the parameters for **1** are similar to those observed for other distorted six-coordinate Co(II) complexes.<sup>7</sup> Complete active space (CAS) calculations were used to substantiate the influence of the structural distortions on the electronic structure of **1** (see Computational

**Scheme 1.** (a) Simplified Energy Level Diagram for the Splitting of the  $^4T_{1g}$  Ground State in the Presence of an External Magnetic Field Parallel to the Easy Axis and (b) Splitting of the d-Type Metal Orbitals of an Ideal Octahedral High-Spin Co<sup>II</sup> Ion ( $d^7$ ) after the Application of a Rhombic ( $C_{2v}$ ) Distortion (Gray Arrows)



Details in the SI). The CAS calculations established the energy order of the 3d orbitals shown in Scheme 1 (Figure S6) and unambiguously supported the positive sign of  $\Delta$ , whose calculated magnitude was in agreement with the experimental one (see the SI for a detailed discussion). Second-order SOC splits the  $S = 3/2$  spin quadruplet into two Kramers doublets ( $M_S = \pm 1/2$  and  $\pm 3/2$ ) separated by an energy gap equal to  $2D$ . When  $\Delta > 0$ , it is also true that  $D > 0$ , that is, the  $M_S = \pm 1/2$  doublet is the ground state.

To determine the magnitude and sign of the  $D$  parameter, field-dependent magnetization data and electron paramagnetic resonance (EPR) spectra at low temperatures were measured (Figures S5 and S8). The low-temperature experimental magnetization data of **1** were then analyzed using VPMAG<sup>8</sup> with the appropriate spin Hamiltonian,  $\hat{H} = D[\hat{S}_z^2 + S(S+1)/3] + E(\hat{S}_x^2 + \hat{S}_y^2) + \beta g \mathbf{H} \cdot \hat{S}$ , which takes into account the axial ( $D$ ) and rhombic ( $E$ ) magnetic anisotropies. The best-fit values of the parameters were  $D = +98 \text{ cm}^{-1}$ ,  $E = +8.4 \text{ cm}^{-1}$ , and  $g = 2.78$  with  $R = 1.3 \times 10^{-5}$  (solid lines in Figure S5).

The polycrystalline powder X-band EPR spectrum at 8.0 K presented rhombic symmetry with  $g_x = 6.1$ ,  $g_y = 3.8$ , and  $g_z = 2.4$  (Figure S8). This pattern of the  $g$  values ( $g_x, g_y > g_z$ ) is characteristic of an orbitally nondegenerate ground state ( $\Delta > 0$ ) with a large positive  $D$  value.<sup>9</sup> CAS calculations also showed a large, positive  $D$  value ( $D = +146 \text{ cm}^{-1}$ ) with a significant rhombicity ( $E/D = 0.185$ ). In addition, the calculated  $g$  values ( $g_x = 6.3$ ,  $g_y = 4.3$ , and  $g_z = 2.4$ ) were in agreement with the experimental ones (see Computational Details).

The alternating-current (ac) magnetic susceptibility of **1** was then investigated under different applied static fields in the range 0–1.0 kG, and Figure 2 shows the results in the form of plots of  $\chi'_M$  and  $\chi''_M$  versus  $T$ , where  $\chi'_M$  and  $\chi''_M$  are the in-phase and out-of-phase ac magnetic susceptibilities per mononuclear unit. Although no  $\chi''_M$  signals were observed under zero dc magnetic field even at the highest frequency used ( $\nu = 10 \text{ kHz}$ ), nonzero  $\chi''_M$  signals appeared when a small static dc field (e.g., 0.1 kG) was applied (Figure 2b). Moreover, under an applied field of 1.0 kG, strong frequency-dependent maxima in both  $\chi'_M$  and  $\chi''_M$  occurred below 10 K (Figure 2). Nevertheless, fast tunneling relaxation at low temperatures was still present at 1.0 kG, as marked by the divergence in  $\chi''_M$  below the blocking temperature (Figure 2b). This behavior, which has been observed previously for other SMMs,<sup>1,6</sup> implies that the superparamagnetic blocking is achieved only at high frequencies because of the fast zero-field quantum-tunneling relaxation of the magnetization. Additional ac measurements on **1** under

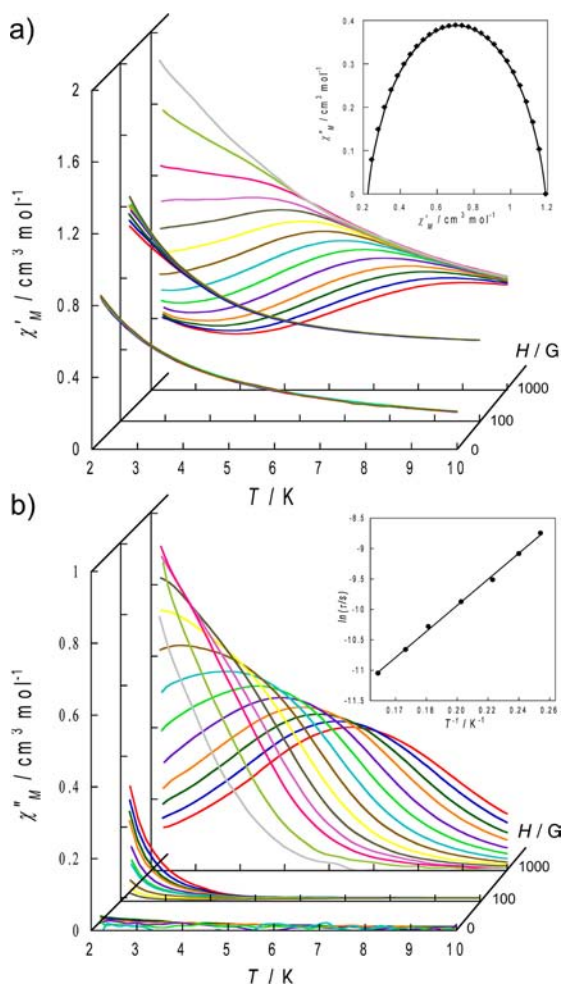


**Figure 2.** Temperature dependence of (a)  $\chi_M'$  and (b)  $\chi_M''$  of **1** under static applied dc fields of 0, 0.1, and 1.0 kG with a  $\pm 4.0$  G oscillating field at frequencies in the range of (gray) 0.1 to (red) 10 kHz. The inset in (a) shows the Cole–Cole plot at 6.0 K, and that in (b) shows the Arrhenius plot in the high-temperature region under a static applied field of 1.0 kG.

higher applied dc fields of 2.5 and 5.0 kG showed that the fast tunneling relaxation at low temperatures disappeared, as evidenced by the single strong frequency-dependent  $\chi_M''$  maximum below 10 K (Figures S9b and S10b).

The Cole–Cole plots for **1** at 6.0 K under different applied dc fields of 1.0, 2.5, and 5.0 kG gave almost perfect semicircles that were fit using the generalized Debye model (solid lines in the insets of Figure 2a and Figures S9a and S10a).<sup>10a</sup> The calculated low values of the  $\alpha$  parameter under the different applied dc fields ( $\alpha = 0.07$ – $0.14$ ; Table S2 in the SI) support a single relaxation process and thus discard spin-glass behavior ( $\alpha = 0$  for a Debye model).<sup>10b</sup> Moreover, the values of the relaxation time ( $\tau$ ) of **1**, which were calculated from the maximum of  $\chi_M''$  at a given frequency [ $\tau = (2\pi\nu)^{-1}$ ], followed the Arrhenius law [ $\tau = \tau_0 \exp(E_a/k_B T)$ ], characteristic of a thermally activated mechanism (solid lines in the insets of Figure 2b and Figures S9b and S10b). The calculated values of the pre-exponential factor [ $\tau_0 = (3.0$ – $4.4) \times 10^{-7}$  s] and the activation energy ( $E_a = 16.2$ – $18.1$  cm<sup>-1</sup>) (Table S2) are consistent with those previously reported for the very few other Co(II) SIMs having tetrahedral<sup>6a,b</sup> and square-pyramidal<sup>6c</sup> geometries.

To obtain further confirmation of the unique field-induced slow magnetic relaxation behavior of **1**, additional dc magnetization measurements at very low temperatures in the range 0.03–1.3 K and field-sweep rates varying in the range 0.004–0.280 T s<sup>-1</sup> were performed on single crystals of **1** using a micro-SQUID (Figure 3 and Figure S11). The observed

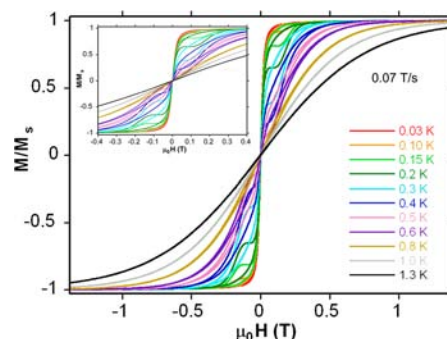


**Figure 3.** Field dependence of the normalized magnetization of **1** over the temperature range 0.03–1.3 K (field-sweep rate = 0.07 T s<sup>-1</sup>). The inset shows the hysteresis loops in detail.

hysteresis loops were strongly dependent on the temperature and the field-sweep rate, as found for related polynuclear SMMs.<sup>4</sup> At zero dc field, however, fast quantum tunneling of the magnetization led to a very closed hysteresis loop, in agreement with the ac magnetic susceptibility measurements. Thus, at the lowest temperature of 30 mK, the hysteresis practically disappeared because of the fast ground-state tunneling (Figure 3 inset).

In principle, it is not easy to understand how a molecule with a positive anisotropy ( $D > 0$ ) can exhibit SMM behavior. In general, a positive  $D$  value and slow magnetic relaxation processes are commonly regarded as being antagonistic. In this sense, even for a negative  $D$  value, the classical rotation of the magnetic moment from  $M_S = +3/2$  to  $-3/2$  would require an energy barrier of  $E_a = 2|D| = 196$  cm<sup>-1</sup>, a value which is 1 order of magnitude greater than that experimentally observed, ( $E_a \approx 17.0$  cm<sup>-1</sup>). Consequently, a new physics implying a smaller energy barrier must be involved. The origin of this barrier could be governed by a transverse anisotropy ( $xy$  easy plane) instead of the usual axial one ( $z$  easy axis).

The  $M_S = \pm 1/2$  component has minimum and maximum spin projections along the  $z$  axis and the  $xy$  plane, respectively. On the other side, the opposite situation accounts for the  $M_S = \pm 3/2$  component. For a purely axial symmetry, the spin has no preferred orientation within the  $xy$  easy plane ( $D_{xx} = D_{yy}$ ). However, the situation could be quite different when a transverse anisotropy of the form  $E(\hat{S}_x^2 - \hat{S}_y^2)$  is present, where  $E = (D_{xx} - D_{yy})/2$ . In such a case, this transverse anisotropy would create a preferred axis within the  $xy$  plane. This easy axis would lie along either the  $x$  or  $y$  direction, depending on the sign of  $E$ , and a highly anisotropic energy barrier would prevent the rotation of the moment from  $+x$  (or  $+y$ ) to  $-x$  (or  $-y$ ). It is important to note that the maximum barrier height corresponding to the rotation of the moment through the  $z$  axis would be dictated by  $D = 3D_{zz}/2$ , while the barrier height corresponding to rotation within the  $xy$  plane would be controlled by  $E$ . Since  $E \leq D/3$ , a transverse barrier would be always smaller than an axial one. In our case, the theoretical axial anisotropy barrier ( $2|D| = 196$  cm<sup>-1</sup>) obtained from the experimental  $D$  value is in total disagreement with the

experimental barrier of ca.  $17.0 \text{ cm}^{-1}$ . However, the energy of the transverse barrier for rotation in the  $xy$  plane, given by  $2E = D_{xx} - D_{yy}$ , provides an energy barrier of  $E_a = 2E \approx 16.8 \text{ cm}^{-1}$  (from the experimental  $E$  value of  $8.4 \text{ cm}^{-1}$ ) which is very close to the experimental one. This fact strongly supports the idea that the transverse anisotropy energy barrier could be responsible for the slow magnetic relaxation behavior in **1**. Moreover, for an  $M_S = \pm 1/2$  Kramers doublet ground state, the quantum-tunneling effects may prevent localization of the molecular magnetic momentum within the  $xy$  plane ( $\langle S_x \rangle = \langle S_y \rangle = 0$ ). Hence, no slow magnetic relaxation should be expected unless the tunneling effects are suppressed by the application a dc external magnetic field, as observed in **1**.

Very recently, Long and co-workers suggested for the first time this transverse anisotropy barrier ( $E$ ) as a possible source of slow magnetic relaxation behavior in a single-chain magnet.<sup>11</sup> In another recent study, the same group also reported the occurrence of slow magnetic relaxation in a tetrahedral Co(II) complex with easy-plane anisotropy ( $D > 0$ ).<sup>6c</sup> In this case, however, a field-induced bottleneck of the direct relaxation between the  $M_S = \pm 1/2$  levels generated Orbach relaxation pathways through the excited  $M_S = \pm 3/2$  levels, with the barrier to spin relaxation still being controlled by  $D$  in spite of its positive sign.

In conclusion, we have reported the first example of a six-coordinate mononuclear Co(II) complex that behaves as an SIM, with the few other examples of Co(II) SIMs reported in the literature being four- or five-coordinated species. The large rhombic distortion of the octahedral environment of the Co<sup>II</sup> ion in **1**, which is likely due to the sterically hindered nature of the dmphen ligands, is responsible for the large and positive value of the axial magnetic anisotropy ( $D > 0$ ) and the non-negligible rhombicity ( $E/D \neq 0$ ), as confirmed by magnetization measurements, EPR spectroscopy, and theoretical calculations. More importantly, **1** represents the first SIM for which field-induced slow magnetic relaxation does not arise from the axial anisotropy energy barrier controlled by the  $D$  parameter but instead is due to a transverse anisotropy energy barrier governed by the  $E$  parameter. This is an unprecedented phenomenon in molecular nanomagnetism, and it represents a potentially new design strategy leading toward the construction of a new class of SMMs. Future efforts will be devoted to the development of other six-coordinate mononuclear Co(II) SIMs with large positive  $D$  values and significant  $E$  values in order to confirm this new physics.

## ■ ASSOCIATED CONTENT

### ■ Supporting Information

Preparation details; analytical and additional structural, spectroscopic, and magnetic characterization data; and computational details for **1**. This material is available free of charge via the Internet at <http://pubs.acs.org>.

## ■ AUTHOR INFORMATION

### Corresponding Author

joan.cano@uv.es; emilio.pardo@uv.es

### Notes

The authors declare no competing financial interest.

## ■ ACKNOWLEDGMENTS

This work was supported by the MICINN (Spain) (Project CTQ2010-15364), the University of Valencia (Project UV-

INV-AE11-38904), and the Generalitat Valenciana (Spain) (Projects PROMETEO/2009/108, GV/2012/051, and ISIC/2012/002). J.V. and E.P. thank the MICINN for contracts.

## ■ REFERENCES

- (1) (a) Ishikawa, N.; Sugita, M.; Ishikawa, T.; Koshihara, S.-Y.; Kaizu, S. *J. Am. Chem. Soc.* **2003**, *125*, 8694. (b) Ishikawa, N.; Sugita, M.; Ishikawa, T.; Koshihara, S.; Kaizu, S. *J. Phys. Chem. B* **2004**, *108*, 11265. (c) Rinehart, J. D.; Long, J. R. *J. Am. Chem. Soc.* **2009**, *131*, 12558. (d) Rinehart, J. D.; Meihaus, K. R.; Long, J. R. *J. Am. Chem. Soc.* **2010**, *132*, 7572. (e) Layfield, R. A.; McDouall, J. J. W.; Sulway, S. A.; Tuna, F.; Collison, D.; Winpenny, R. E. P. *Chem.—Eur. J.* **2010**, *16*, 4442. (f) Car, P.-E.; Perfetti, M.; Mannini, M.; Favre, A.; Caneschi, A.; Sessoli, R. *Chem. Commun.* **2011**, 47, 3751. (g) Jeletic, M.; Lin, P.-H.; Le Roy, J. J.; Korobkov, I.; Gorelsky, S. I.; Murugesu, M. *J. Am. Chem. Soc.* **2011**, *133*, 19286. (h) Chen, G.-J.; Guo, Y.-N.; Tian, J.-L.; Tang, J.; Gu, W.; Liu, X.; Yan, S.-P.; Cheng, P.; Liao, D.-Z. *Chem.—Eur. J.* **2012**, *18*, 2484. (i) Vallejo, J.; Cano, J.; Castro, I.; Julve, M.; Lloret, F.; Fabelo, O.; Cañadillas-Delgado, L.; Pardo, E. *Chem. Commun.* **2012**, 48, 7726.
- (2) Winpenny, R. E. P. *Adv. Inorg. Chem.* **2001**, *52*, 1.
- (3) Gatteschi, D.; Sessoli, R. *Angew. Chem., Int. Ed.* **2003**, *42*, 268.
- (4) Gatteschi, D.; Sessoli, R.; Villain, J. *Molecular Nanomagnets*; Oxford University Press: Oxford, U.K., 2006.
- (5) (a) Freedman, D. E.; Harman, W. H.; Harris, T. D.; Long, G. J.; Chang, C. J.; Long, J. R. *J. Am. Chem. Soc.* **2010**, *132*, 1224. (b) Harman, W. H.; Harris, T. D.; Freedman, D. E.; Fong, H.; Chang, A.; Rinehart, J. D.; Ozarowski, A.; Sougrati, M. T.; Grandjean, F.; Long, G. J.; Long, J. R.; Chang, C. J. *J. Am. Chem. Soc.* **2010**, *132*, 18115. (c) Weismann, D.; Sun, Y.; Lan, Y.; Wolmershäuser, G.; Powell, A. K.; Sitzmann, H. *Chem.—Eur. J.* **2011**, *17*, 4700. (d) Lin, P.-H.; Smythe, N. C.; Gorelsky, S. I.; Maguire, S.; Henson, N. J.; Korobkov, I.; Scott, B. L.; Gordon, J. C.; Baker, R. T.; Murugesu, M. *J. Am. Chem. Soc.* **2011**, *133*, 15806.
- (6) (a) Zadrozny, J. M.; Long, J. R. *J. Am. Chem. Soc.* **2011**, *133*, 20732. (b) Jurca, T.; Farghal, A.; Lin, P.-H.; Korobkov, I.; Murugesu, M.; Richardson, D. S. *J. Am. Chem. Soc.* **2011**, *133*, 15814. (c) Zadrozny, J. M.; Liu, J.; Piro, N. A.; Chang, C. J.; Hill, S.; Long, J. R. *Chem. Commun.* **2012**, 48, 3927.
- (7) Lloret, F.; Julve, M.; Cano, J.; Ruiz-García, R.; Pardo, E. *Inorg. Chim. Acta* **2008**, *361*, 3432.
- (8) Cano, J. *VPMAG*; University of Valencia: Valencia, Spain, 2003.
- (9) Banci, L.; Bencini, A.; Benelli, C.; Gatteschi, D.; Zanchini, C. *Struct. Bonding* **1982**, *52*, 37.
- (10) (a) Cole, K. S.; Cole, R. H. *J. Chem. Soc.* **1941**, 9, 341. (b) Mydosh, J. A. *Spin Glasses: An Experimental Introduction*; Taylor & Francis, London, 1993.
- (11) Feng, X.; Liu, J.; Harris, T. D.; Hill, S.; Long, J. R. *J. Am. Chem. Soc.* **2012**, *134*, 7521.